HAL
open science

Energy requirements to produce fine powders of raw and torrefied wood at pilot scale, and characterization of their flowability

Florent Thevenon, Muriel Marchand, Maguelone Grateau, Hary Demey, André Chatroux, Philippe Pons de Vincent, Alain de Ryck, Thierry Melkior

To cite this version:

Florent Thevenon, Muriel Marchand, Maguelone Grateau, Hary Demey, André Chatroux, et al.. Energy requirements to produce fine powders of raw and torrefied wood at pilot scale, and characterization of their flowability. Biomass and Bioenergy, 2021, 152, pp.1-14/106196. 10.1016/j.biombioe.2021.106196 . hal-03306896

HAL Id: hal-03306896

https://imt-mines-albi.hal.science/hal-03306896v1

Submitted on 29 Jul 2021

HAL is a multi-disciplinary open access archive for the deposit and dissemination of scientific research documents, whether they are published or not. The documents may come from teaching and research institutions in France or abroad, or from public or private research centers.

L'archive ouverte pluridisciplinaire **HAL**, est destinée au dépôt et à la diffusion de documents scientifiques de niveau recherche, publiés ou non, émanant des établissements d'enseignement et de recherche français ou étrangers, des laboratoires publics ou privés.

Energy requirements to produce fine powders of raw and torrefied wood at pilot scale, and characterization of their flowability

Florent Thevenon [a,b,c,*], Muriel Marchand [a], Maguelone Grateau [a], Hary Demey [a], André Chatroux [a], Philippe Pons de Vincent [a], Alain De Ryck [b], Thierry Melkior [a]

[a] Université Grenoble Alpes, CEA, LITEN, DTCH, LRP, F-38000, Grenoble, France
[b] Centre RAPSODEE, UMR CNRS 5302, IMT Mines Albi, Campus Jarlard, Albi Cedex 09, 81013, France
[c] Agence de l'Environnement et de la Maîtrise de l'Energie, 20 avenue du Grésillé - BP 90406, Angers Cedex 01, 49004, France

Keywords:
Biomass
Torrefaction
Vibration mill
Energy assessment
Powder flowability
Post-combustion

A B S T R A C T

This work aims at comparing different preparation chains to produce wood powders suitable for further gasification in an entrained flow reactor. Three wood powders, with particle size below 1 mm, have been produced at pilot scale from resinous wood chips: a powder of raw wood and a powder of torrefied wood both ground in a knife mill, and a powder of raw wood ground in a vibration mill. The respective requirements both in energy and in feedstock material resource have been determined for each chain of production. The production of the raw wood powder requires 0.83 MWh per ton of dry powder (tdp). The additional grinding step with the vibrating mill adds 0.63 MWhel.tdp^{-1}. The production of the torrefied wood powder requires 3.56 MWh.tdp^{-1}. Moreover, the wet wood chips requirements vary from 2.5 tons for the chains of production without torrefaction to 4.4 tons for the chain including a torrefaction step. In the latter, the step with the highest energy demand is the gas-cleaning step in an instrumented post-combustion reactor. Heat recovery from the combustion gases could supply energy to both the drying and torrefaction steps. It would reduce by half the total energy cost of the chain, down to 1.66 MWh.tdp^{-1}. The resource requirements would be reduced down to 3.2 tons. The morphology and flowability of the powders have been investigated and compared. Torrefaction or vibration milling significantly improve the ability of the wood powder to flow both without any stress or when consolidated by a vertical stress.

1. Introduction

To limit the global warming, it is crucial to reduce the energy consumption and to develop renewable energies. According to the International Energy Agency (IEA), biofuels account for nearly 10 % of world total primary energy supply in 2017 [1]. Heat, electricity, bio-based chemicals, bio-based materials or also biofuels can be produced from biomass via a wide number of routes. Actual first-generation biofuels are produced via biological or chemical processes such as fermentation for ethanol production or transesterification for diesel but are coming under increasing criticism. Indeed, these processes operate with agricultural biomass which is in competition with food use. Current researches are focused on the production of second generation biofuels from lignocellulosic biomass via saccharification, liquefaction or gasification [2]. Gasification is a thermal conversion of biomass to produce a syngas which can further be converted into biofuels via Fischer-Tropsch synthesis.

Gasification of biomass can be performed in different technologies of reactor such as fixed bed reactor, fluidized bed reactor or entrained flow reactor (EFR). Gasification in EFR requires to process biomass as a fine powder. Indeed, residence time of solid particles inside this kind of reactor is a few seconds, and the full conversion of the solid can only be achieved if the particles are small enough. Consequently, biomass has to be milled prior to be gasified in such reactor. It has been previously shown that woody particles as small as 1000 μm are fully converted at 1300 °C in a pilot-scale EFR [3]. However, according to a review published by Karinkanta et al., fine grinding of wood is highly energy consuming, from 100 to 1000 kWh.t^{-1} [4]. Moreover, the interparticle forces between fine particles (smaller than 100 μm) exceed the gravitational forces [5]. The bulk density of wood powder could be as weak as 150 kg.m^{-3} [6]. Lastly, the particles of wood powder could be elongated [7]. These characteristics result in frequent issues of handling wood powder. For instance, the powder may form arches in hopper [6], which is a major concern in industrial applications.

* Corresponding author. CEA, LITEN, DTCH, LRP, F-38000, Grenoble, France.
E-mail address: florent.thevenon@mines-albi.fr (F. Thevenon).

Ambrose et al. defined the flowability of a powder as its capacity to move by flow under a specified set of stresses [8]. Several characterization methods exist to assess the flowability of powders, depending on their stress state [9]. Dynamic flow of cohesive bulk solids under very low stresses can be characterized in a rotating drum [10–12]. This apparatus is useful to study the avalanching dynamics of a powder. In an industrial plant, powders are generally in unconfined state during conveying and discharge from a screw feeder. Furthermore, shear cells are commonly used to characterize the powder flowability under high normal stresses. The powder is therefore in a comparable state of consolidation as a powder stuck in an industrial hopper [13].

Torrefaction is a promising process to pretreat biomass before its conversion in gasification or co-combustion processes [14–16]. It is a thermal pretreatment, which takes place between 220 and 300 °C, under inert atmosphere during a few dozen of minutes. The properties of biomass after torrefaction are closer to that of coal. The carbon content of the solid is increased, as well as its energy density and hydrophobicity. It makes biomass transportation more feasible. Torrefaction improves the material resistance to fungal degradation [17,18], improves the conversion of biomass into syngas during the gasification process [19–21], as well as its combustion [22,23]. Furthermore, it is a very efficient treatment to reduce the energy requirements of fine grinding of biomass [24–27]. Lastly, it improves the fluidization and flowability properties of biomass powders [28–30] at the expense of a supplementary unit operation and energy costs.

The brittleness of torrefied biomass increases with the heat treatment intensity [31]. More severe it is, less energy costly the grinding is [32] and better the flowability is [29]. The grinding energy savings are not proportional to the anhydrous weight loss [25]. The nonlinear relationship between improved grindability and torrefaction severity could arise from the two-step mechanism of hemicelluloses decomposition [24]. The first step is relatively fast, whereas the second one goes more slowly [33]. For instance, the grindability of cedarwood increases sharply with temperature for torrefaction temperatures below 260 °C and increases to a lesser extent for torrefaction temperatures above 260 °C [22]. A compromise has to be found between maintaining a good energy yield and reducing grinding energy. Repellin et al. reported an optimal value of the mass loss of nearly 8 % for woody biomass [25]. Chen et al. recommended a torrefaction treatment at 250 °C during more than 1 h for woody biomass (Lauan) blocks to increase the heating value and the grindability while avoiding too much mass loss [34].

Although the benefits of torrefaction on the grinding energy have been deeply investigated by many authors, only few studies have focused on its own energy cost. Experimental pilot scale data can provide relevant data for upscaling at industrial scale [35]. However, experimental data are scarce in the literature [35–38]. Nanou et al. experimentally studied the torrefaction at 260 °C of moist spruce (45 %) at pilot scale. They reported an energy requirement for predrying plus torrefaction of nearly 1000 $kWh.ton^{-1}$ of dry biomass [35]. Doassans-Carrère et al. studied the torrefaction of biomass with a Vibrating Electrical Elevator and Reactor (REVE). Their experimental results showed that torrefaction between 230 °C and 250 °C of dry wood chips (initial moisture between 10 % and 15 %) required 250 $kWh.t^{-1}$ [36]. Thevenon et al. produced mildly torrefied resinous chips (250 °C for 55 min) in a multiple-hearth furnace (MHF). The whole chain of preparation, also including the drying step and the gas cleaning step downstream the torrefaction, required 3.51 MWh per ton of product [37]. According to Ciolkosz et al. the compensation of the energy cost of torrefaction via reduced cost and/or increased performance in other parts of the process requires more attention to better assess the net benefit of torrefaction [38].

Vibration mills can be used for fine grinding of biomass in processes such as enzyme saccharification or gasification [4,39–41]. Grinding media mills such as vibratory mills involve impacts between particles and solid media such as balls or rods. Vibration mills pulverize biomass in more spherical particles than cutter mill [39]. As round shaped particles flow better than elongated particles, this technology of grinders could be an alternative to torrefaction, provided that its cost is also competitive. In vibration mills, the size reduction is caused by the impacts between a particle and two solid bodies [4]. Karinkanta et al. studied the fine grinding of spruce wood with an oscillatory ball mill [42] and suggest that grinding media mills cause more changes in particle shape because the nature of impacts results in higher energy expended on morphological changes than with rotor impacts. Furthermore, the acceleration of a particle after an impact with a grinding medium is very low, whereas in rotating tools grinders (like knife or hammer mill), after impacting another particle or the moving tool, the particle is accelerated. This acceleration dissipates a part of the impact energy [42]. Vibratory mills consume a large amount of energy [39,41]. Kobayashi et al. reported a total energy consumption of 800 $kWh.t^{-1}$ for continuous pulverization of wood chips from 22 mm to 150 μm [39].

In this work, the total energy requirements are determined for four different preparation chains aimed at producing wood powders with particle size below 1000 μm, starting from moist wood chips. The different chains considered here are respectively constituted of the following steps:

- Drying + Grinding (DG)
- Drying + Torrefaction + Grinding (DTG)
- Drying + Torrefaction with Heat integration + Grinding (DTG + Hi)
- Drying + Grinding + Vibration mill (DGV)

The objective of this study is to compare the different chains of production listed above, based on their respective energy requirements, but also based on the powder quality, assessed by its ability to flow. To get the most relevant results, the experimental determination of energy requirements has to be carried out at the largest possible scale. Therefore, pilot scale devices have been used for the preparation of wood powders, from the same batch of raw wood chips. These wood powders all had to have particle size below 1000 μm, to agree with the maximum admissible particle size for a full conversion in EFR [3]. At each step, the energy consumed has been measured, and the mass balance has been determined. Finally, the different powders have been characterized, for their particles sizes and forms, and for their flowabilities.

2. Materials and methods

2.1. Biomass

Biomass examined in this study is a mix of stem and bark from spruce wood (about 70 %) and pine wood (about 30 %). The biomass originates from Goncelin (Isère, France). It is a promising resource around Grenoble (Isère, France), due to its large availability in the Alps. 12 big bags of 1 m^3 each have been supplied. The mean dimensions are 45 (±13.3) * 24 (±5.4) * 7 (±1.9) mm^3. The moisture content of these wood chips has been measured according to the NF-EN- 14.774 standard. A sample of about 40 g has been dried at 105 °C for 24 h. One sample has been collected in each big bag at about 30 cm depth, to avoid sampling the chips located on the top of the bag. The averaged moisture content of wood chips is found to be 52 % on wet basis, with a standard deviation of 2.6 %. It is concluded that the moisture content is homogeneous, and that the averaged value will thereafter be used for all the bags.

The C, H, N, S and O contents of the raw biomass have been measured with an averaged sample made of a mix of a dozen of wood chips collected in each big bag. C, H, N, and S contents have been measured with a Vario EL cube instrument (ELEMENTAR, Langenselbold, Germany). The ash content has been measured according to the XP CEN/TS 14775 (combustion at 550 °C). The oxygen content has been obtained by difference after determination of the C, H, N, S, and ash contents. The higher heating value (HHV) has been measured using a 6200 isoperibol oxygen bomb calorimeter (PARR, Moline-Illinois, USA) with a sample of about 1 g of dried biomass. More details about the procedures that have

been used for these measurements can be found in Ref. [37].

Elemental analysis and HHV of the raw wood are presented in Table 1, on a dry basis.

2.2. Pilot scale facilities

The different pilots that have been used for this work all belong to the biomass research platform of CEA (Grenoble, France). As the dryer and the torrefaction furnace are thoroughly presented elsewhere [37,43,44], only the main aspects are reminded hereafter.

2.2.1. Drying

Due to the high moisture content of biomass as supplied, a drying step is required prior to any further operation. Wood moisture content must be kept below 20 % on wet basis (%wb) to prevent it from decay [45]. Drying has been achieved using a continuous two floors belt dryer provided by SCOLARI (Paderno, Italy). This equipment is swept at counter-current with air pre-heated by a natural gas burner. The inlet flow rate of biomass has been set at 120 kg.h^{-1} on wet basis. The flow rate of biomass has been calculated from the measured residence time of the chips inside the dryer and the wood chips density:

$$\dot{F}_{biomass} = \left(L_{dryer} / \tau_{residence} \ {}^{*}l_{dryer} {}^{*}h_{bed}\right) {}^{*}\rho_{biomass} \left(kg.s^{-1}\right) \quad (1)$$

where L_{dryer} is the total length of the two conveyors (6.2 m), $\tau_{residence}$ is the residence time of the chips inside the drying plant (4680 s), l_{dryer} is the width of the conveyor (0.85 m), h_{bed} is the height of the biomass bed (0.1 m) and $\rho_{biomass}$ is the bulk density of wood chips, either the moist wood chips or the dried wood chips. The inlet and outlet flow rates have been calculated respectively using the measured density of wood chips before drying (289 kg.m^{-3}) and shortly after drying (185 kg.m^{-3}). As no biomass accumulation was observed in the dryer, the flow rate of evaporated water has been calculated as the difference between inlet and outlet flow rates of biomass.

The flow rate of natural gas used to heat the air which is injected into the dryer has been monitored during steady state operation. It allows the calculation of the burner power:

$$P_{burner} = \left(\dot{V}_{natural\ gas} LHV_{natural\ gas}\right) \Big/ 3.6(kW) \quad (2)$$

where $\dot{V}_{natural\ gas}$ is the flow rate of natural gas injected into the burner (Nm^3.h^{-1}). The mean lower heating value (LHV) of natural gas in France (excepted in the North region) is 41.04 MJ.Nm^{-3}.

2.2.2. Torrefaction

Torrefaction of wood chips has been performed in a vertical six hearths furnace provided by CMI Group. The total height of the furnace is about 10 m, and the internal diameter is 1.82 m. The height of each hearth is 0.74 m (Fig. 1). Each stage is heated up by two direct-fired natural gas burners. A rabbling system, moved by the central shaft (i. d. Ø 0.42 m), transfers the wood chips through the hearths. After exiting the furnace, the torrefied wood chips are cooled down inside two successive cooled screw conveyors and collected in containers of 1 m^3, maintained under inert conditions. The torrefaction facility is instrumented, to provide all the data required to establish mass and energy balances.

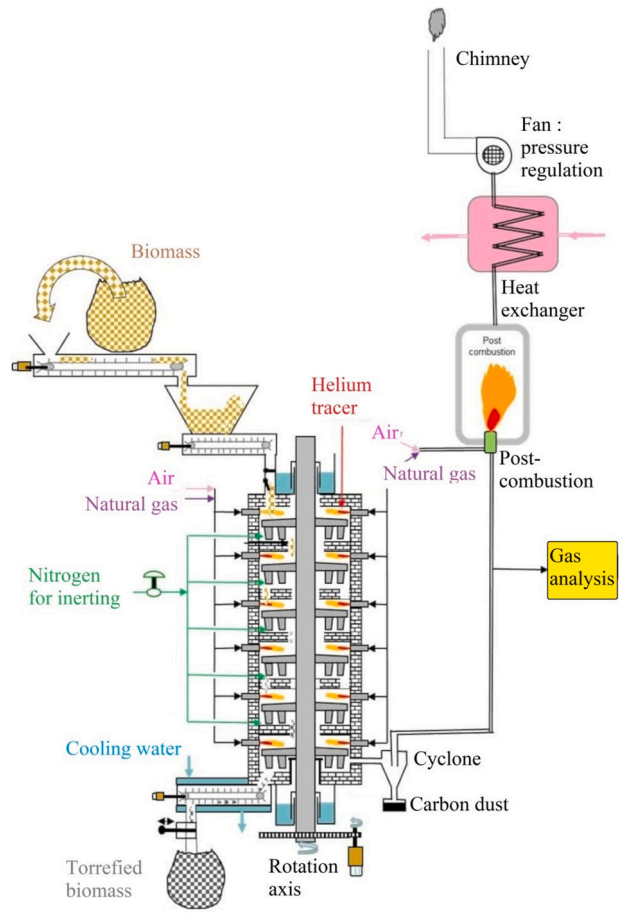

Fig. 1a. Synoptic of the torrefaction unit.

In this study, torrefaction has been carried out at 250 °C for 55 min. Chen et al. recommended a torrefaction treatment at 250 °C during more than 1 h for woody biomass (Lauan) blocks to increase the heating value and the grindability while avoiding too much mass loss [34]. A torrefaction process simulation developed by Maski et al. revealed that for a biomass moisture of 10–20 %, the torrefaction process should be carried out at a temperature between 240 and 260 °C in order to minimize the energy cost while maximizing the torrefied solid yield [46]. Thus, a mildly temperature (temperature of 250 °C), even with a quite long residence time, seems to be optimal. The inlet flow rate of biomass has been set at 65 kg.h^{-1}. Torrefaction has been completed after 8h30 of total operating time over two days (denoted T1 and T2 afterwards). About 420 kg of torrefied material have been produced.

The mass yield η_m is expressed on a dry basis as the percentage of the dry raw biomass that is recovered in the torrefied solid:

$$\eta_m = \dot{F}_{biomass,outlet,T} \Big/ \left(\dot{F}_{biomass,inlet,T}(1 - H_i)\right)(\%) \quad (3)$$

where $\dot{F}_{biomass,inlet,T}$ is the inlet flow rate of biomass (65 kg.h^{-1}), H_i is the moisture content of the inlet biomass (11 %) and $\dot{F}_{biomass,outlet,T}$ is the

Table 1
Properties of the raw and torrefied resinous wood chips (all values on dry basis). Standard deviations are indicated between parentheses.

Biomass	Chips size reduction			Yields		Elemental analysis						Energy content
	Length (%)	Width (%)	Thickness (%)	Mass (%)	Energy (%)	C (%)	H (%)	O (%)*	N (%)	S (%)	Ash (550 °C) (%)	HHV (MJ.kg^{-1})
Raw	–	–	–	–	–	46.3 (0.08)	6.4 (0.02)	46.8	0.12 (0.00)	0.07 (0.004)	0.3 (0.07)	18.4
Torrefied	13	10	Unchanged	89.6 (0.0)	95.3 (0.0)	49.9 (0.2)	6.5 (0.2)	43.0	0.18 (0.01)	0.05 (0.021)	0.4 (0.02)	19.5

*By difference.

Fig. 1b. Picture of the torrefaction unit (Dominique GUILLAUDIN/CEA (Malverpix No Comment Studio)).

outlet flow rate of biomass (52 kg.h^{-1}).

The torrefied wood chips have been analyzed according to the methods described in section 2.1. The results of ultimate analyses are presented in Table 1.

The energy yield η_e is calculated as the percentage of the energy contained in the dry raw biomass that is recovered in the torrefied wood:

$$\eta_e = \eta_m * \left(LHV_{torrefied\ \ biomass}\right) / \left(LHV_{raw\ \ biomass}\right)(\%) \quad (4)$$

where $LHV_{raw\ biomass}$ and $LHV_{torrefied\ biomass}$ are respectively the lower heating values of raw and torrefied wood (MJ.kg^{-1}).

In order to determine the energy cost of torrefaction, the thermal power supplied by the 12 burners has been calculated according to eq. (2).

A small fraction of the outlet gases stream has been sampled for analysis in a gas line, kept at 200 °C thanks to heating flex to prevent condensation of tars upstream the cold traps. The gas composition has been analyzed thanks to a micro Gas Chromatograph (μGC). The following compounds can be quantified: He, H_2, O_2, N_2, CH_4, CO, CO_2, C_2H_2, C_2H_4, C_2H_6, C_3H_8, H_2S and COS. An analysis is performed every 3 min and the lower limit of quantification is 3 ppm for each gas.

2.2.3. Post-combustion and heat exchanger

The gases and tars leaving the torrefaction furnace have been burnt at 1000 °C in a post-combustion unit to avoid the emissions of pollutants, as required by the French regulation [47]. Gases are composed of the flue gases from the burners mixed with the gases and condensables produced by torrefaction itself. The post-combustion reactor is heated by a direct-fired natural gas burner, which maintains a temperature of 1000 °C inside the reactor. The power supplied by the burner has been calculated from the measured volumetric flow rate of natural gas according to eq. (2).

Downstream post-combustion, hot flue gases go through a fume/air heat exchanger. The volumetric flow rate of outdoor cold air entering the heat exchanger is adjusted so that the outlet air reaches a temperature between 120 and 150 °C. The temperatures of secondary air both at the inlet and at the outlet of the heat exchanger have been monitored together with its flow rate. These data have been used to calculate how much energy could be recovered.

2.2.4. Grinding

Raw and torrefied wood chips have been ground in a continuous 11 kW knife-mill equipped with a 1 mm screen or a 5 mm screen (FORPLEX, Bethune, France). The motor frequency has been set at 50 Hz, and the electrical power consumption has been continuously monitored. The powder has been collected into a barrel, which is weighed continuously. Prior to the injection of biomass, the empty grinding mill operates during a few minutes to measure the power under no load conditions, found to be 2.5 kW. The measurements have been recorded once the steady state has been established.

The comminution of the raw wood in the grinder equipped with a 1 mm screen could not be performed properly due to recurrent blockages of wood chips before entering the grinding chamber. Thus, the steady state was not achieved during experiments performed with those conditions. Furthermore, the resulting powder was containing many fine particles (61 % of particles were smaller than 100 μm). The small particles (<100 μm) have a relatively high surface area to volume ratio, which increases the significance of the attractive forces between particles and thus the cohesion of the powder [9,48]. Following these considerations, it has been decided to use a 5 mm screen instead. For each material, three replicates have been carried out and about 20 kg of each powder have been produced in total.

The rotation speed of the knives has been set at the same value for raw and torrefied wood chips, to have the same impacts on the wood particles. The feeding rate of the grinder has been adjusted to have a similar motor speed, whatever the nature of the wood. The inlet flow rate of torrefied chips has reached 181 kg.h^{-1} whereas it has only reached 59 kg.h^{-1} with the chips of raw wood (Table A.1).

It is not possible to compare the energy consumption measured during the grinding step with other data from the literature, because there are many parameters which impact the energy consumption. Indeed, the characteristics of the resource such as size and shape, its mechanical strength, its moisture content, etc., have an influence on the energy needed to reduce the particle size. Furthermore, many operating parameters such as the filling ratio of the grinder, the motor regime, and the mill characteristics such as mill type, screen size, etc., also affect the results.

A part of the raw biomass firstly ground at 5 mm has been further ground in a continuous vibratory mill (RITEC, La Seyne-sur-Mer, France) (Fig. 2a). The grinding chamber has been filled with 12 cylindrical rods of 30 mm diameter and 15 cylindrical rods of 20 mm diameter. The use of rods with two different diameters improves the efficiency of the operation, because the voids in between the grinding media are reduced (Fig. 2b). The feeding of this device is ensured by a screw conveyor, which transfers the powder from a hopper to a vertical tube leading to the grinder. As this tube diameter is rather small (i.d. Ø 60 mm, length of about 1.8 m), the particles longer than 4.5 mm contained in the powder of raw wood (10 % in volume) frequently formed arches because of steric hindrance. Therefore, the feeding rate had to be lowered by far to avoid arching in the tube. Here, the inlet flow rate of biomass has been set as low as 1.8 kg.h^{-1}. The output rate of powder and the grinding mill power have been monitored at steady state.

2.2.5. Sieving

Gasification in EFR requires to process biomass as a powder with

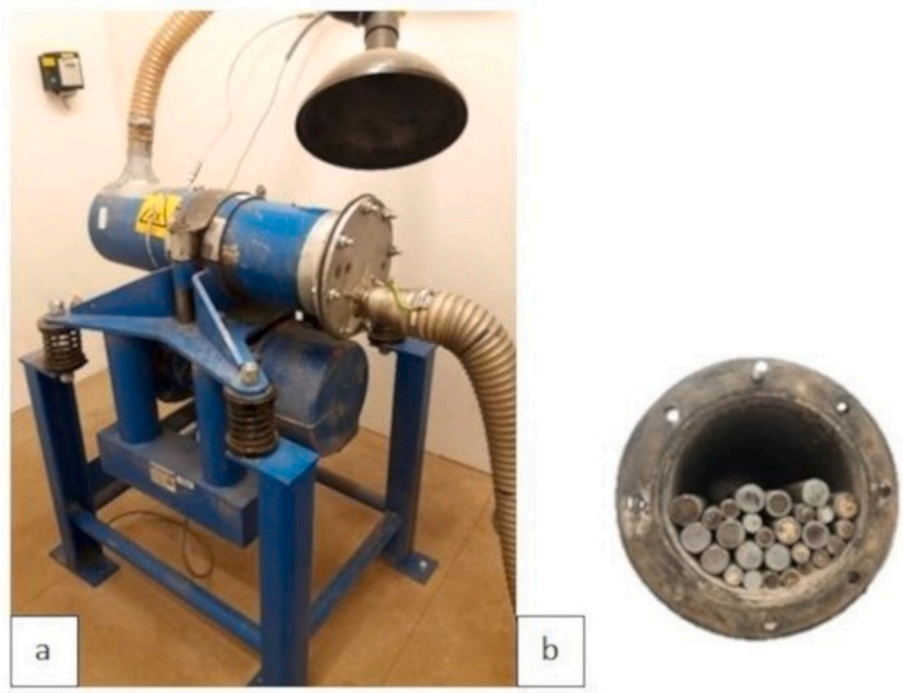

Fig. 2. **(a)** External view of the vibration mill and **(b)** internal view of the grinding chamber. The grinding media, stainless steel rods of two different diameters, can be seen in the chamber.

submillimeter-sized particles. As a 5 mm screen has been used at the outlet of the grinder, a sieving step through a 1 mm sieve has been therefore needed to remove the oversized particles. The sieving has been performed in a sieve shaker.

2.3. Powder characterization

2.3.1. Sampling procedure

A sample of 0.5 kg has been collected for each powder all along the grinding process to ensure the representativeness of the powder sample. The sample has been used for the lab scale characterizations.

2.3.2. Particle morphology

The particle size distribution of each powder has been measured with a dynamic image analyzer (Camsizer XT, RETSCH). The size distribution is given in volume. Four indicators have been considered: the volumetric median diameter (d50), the proportion of particles smaller than 1000 µm, the proportion of particles smaller than 100 µm (content of fines) and the aspect ratio (AR), defined as the ratio of the particle width over its length. The particle width is taken as the minimum chord's diameter, while its length is the maximum Feret's diameter. AR values range between 0 and 1. The measurements have been performed in triplicate.

2.3.3. Rotating drum

The flowability of biomass powders in loose state has been assessed using a REVOLUTION rheometer (MERCURY SCIENTIFIC INC., Newtown, USA). A drum (10 cm diameter, 3.3 cm axial length) containing 79 mL of powder rotates in front of a camera at 0.6 rpm speed. The avalanche angle is defined as the angle between the upper half of the powder surface and the horizontal, just before an avalanche. The smaller the median avalanche angle and the less disperse the distribution are, the better and more regular the unconfined flow is. Variabilities of the feeding rate in screw feeders at time steps longer than 2 s are mainly explained by avalanching problems [49]. Therefore, a powder presenting high avalanche angles in rotating drum is expected to be discharged more erratically from a screw feeder, which is a major issue at industrial scale. The measurement procedure starts by a preparation of the sample during which the drum rotates to erase any operator-induced effects. Once the powder is conditioned, 150 successive avalanches are proceeded, and the retained values are the median and the standard deviation of the avalanche angle distribution. Measurements have been systematically duplicated.

2.3.4. Schulze shear cell

A Schulze annular shear cell (Dietmar Schulze Schüttgutmesstechnik, Wolfenbüttel, Germany) has been used to assess the flow properties of wood powders in consolidated state. The annular shear cell has an external radius diameter of 10 cm, an internal radius diameter of 5 cm and a height of 4 cm. The yield locus has been determined according to the Schulze procedure [50]. It represents the shear resistance of a powder for a given consolidation state. An example of a yield locus curve obtained from shear tests carried out on the coarse torrefied powder is presented in Fig. 3. The procedure is divided in two steps. During the first step, often called "preshear", the sample is consolidated under the preconsolidation stress (σ_c) and it is sheared until steady flow (τ_c). The steady state is reached once the shear stress is constant. The shear stress is then removed by reversing the rotation of the cell during a few seconds, and the normal stress applied on the cell is reduced down to the first value to be tested. The second step, often called "shear", is performed by shearing again the sample at 7 mrad.s^{-1}. The maximum shear stress value τ_s and the corresponding normal stress σ define a shear point of the yield locus (Fig. 3). This two-step procedure is repeated for each point of the yield locus, by increasing gradually the normal stress applied on the powder surface. In this study, the yield loci have been measured at preconsolidation stresses σ_c of 2.7 kPa, 5.3 kPa, 7.9 kPa and 10.5 kPa, which are in the range of stresses applied on powders at the bottom of an industrial hopper. For each preconsolidation test, eight different normal stresses have been successively applied, starting from 0.3 kPa up to the defined preconsolidation stress.

Ideally, the preconsolidation shear stress before each shear test should always be the same. It is not always true. Due to some experimental variations, there is a scatter of values of the pre-shear shear stress

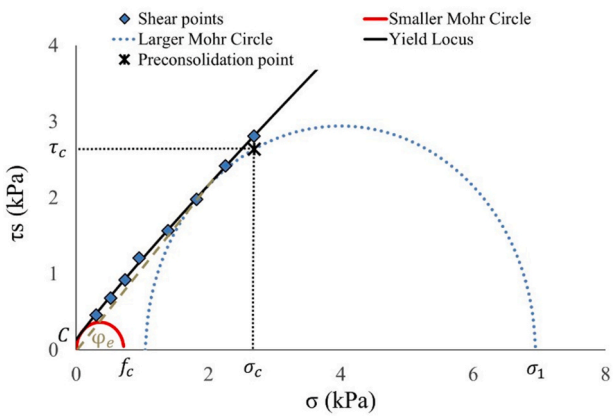

Fig. 3. Example of a yield locus curve generated with the Warren-spring equation. The preconsolidation point, the two Mohr circles describing the Unconfined Yield Strength f_c and the Major Consolidation Stress σ_1, the cohesion C and the effective angle of internal friction ϕ_e are shown. Powder: Coarse torrefied powder. $\sigma_c = 2.7$ kPa.

which affects the value of the shear stress. Prorating has been applied to correct the measured shear stress to minimize the scatter [50]. The prorated values $\tau_s^{'}$ of the measured values τ_s have been evaluated using the following equation:

$$\tau^{'}_{s} = \tau_s * (\tau_{p,m} / \tau_p)(\mathrm{Pa}) \tag{5}$$

where τ_s is the shear stress at yield (Pa), $\tau_{p,m}$ is the average of the pre-shear shear stresses (Pa), τ_p(Pa), of the corresponding pre-shear normal stress level.

The yield locus has been firstly fitted with a Warren-Spring-type equation [51], which is commonly used with cohesive powders such as biomass powders [52]. The Major Consolidation Stress (σ_1) and the Unconfined Yield Strength (f_C) have been obtained for each test by plotting the Mohr circles associated to the fitted Warren-Spring yield locus. The curve $f_C(\sigma_1)$ is called the flow function. The ratio ffc (flow function coefficient) is defined as σ_1/f_C and is used to characterize flowability. The larger ffc is, the better the powder flows. The cohesion C is the shear stress at yield under zero normal stress. It is calculated as the intersection of the yield locus with the shear stress axis. The effective angle of internal friction ϕ_e is defined as the angle between the tangent to the larger Mohr circle passing through the origin in Fig. 3 and the normal stress axis. It is a parameter of interest for the design of the hoppers [53].

2.4. Determination of the energy consumption

The energy consumptions have been determined for each step of preparation. The total energy requirement corresponds to the sum of both thermal and electrical energies used in the process. It has been calculated as the ratio of the total power (P_{total}) over the inlet flow rate ($\dot{F}_{biomass,inlet,db}$), expressed on a dry basis. It has been conventionally expressed in kWh per ton of input biomass on a dry basis (tdb).

$$\mathrm{E_{total}} = \mathrm{P_{total}} \Big/ \dot{\mathrm{F}}_{\mathrm{biomass,inlet,db}} \left(\mathrm{kWh.tdb^{-1}}\right) \tag{6}$$

It is worth noting that the electrical powers needed to operate the dryer, the MHF shaft and the sieve shaker have not been measured.

The net energy consumption has been calculated by subtracting the idle power ($P_{no\ load}$) to the total measured power. It allows an easier comparison of the results with published data, especially for those dealing with grinding. Indeed, the no-load power is non negligible in small-scale grinders, and it varies among the devices [4].

$$\mathrm{E_{net}} = \left(\mathrm{P_{total}} - \mathrm{P_{no\ load}}\right) \Big/ \dot{\mathrm{F}}_{\mathrm{biomass,inlet,db}} \left(\mathrm{kWh.tdb^{-1}}\right) \tag{7}$$

Lastly, the grinding index proposed by Repellin, $E_{<1000\mu m}$, has been used to assess the energy cost of grinding [25]. It divides the energy cost of grinding by the fraction of particles smaller than 1000 μm. This allows to take into account the sieving stage.

$$\mathrm{E_{<1000\mu m}} = \mathrm{E} / (\mathrm{X} < 1000\ \mu\mathrm{m}) \left(\mathrm{kWh.tdb^{-1}}\right) \tag{8}$$

where E is the energy consumption (kWh.tdb^{-1}) and $X < 1000\ \mu m$ is the fraction of particles smaller than 1000 μm, as measured with the size analyzer. Note that the grinding index can be expressed either in net or total basis.

3. Results and discussion

The elementary compositions and energy contents of raw and torrefied woods are presented in Table 1. The total and net energy requirements for each individual step are given in Table 2. The experimental data collected during each step of the preparation of wood powders are summarized in Table A.1 in the appendix A.

3.1. Process properties and results

3.1.1. Drying

The results of the measurements carried out during the drying step and the associated energy requirements are presented in Table A.1 and Table 2 respectively. The inlet and outlet flow rates of biomass are respectively 117 kg.h^{-1} and 75 kg.h^{-1}. The moisture content of biomass has been reduced from 52 % to 18 % (on a wet basis) as targeted.

The total energy consumed for the drying of the wood chips from 52 % to 18 % is 596 kWh.tdb^{-1}. The wood chips, stored into the (opened) big bags under a roof, naturally dried from 18 % to 11 % in contact with air. The energy required for that further drying step has been estimated to be 68 kWh.tdb^{-1}, by theoretical calculations. More details about the drying step can be found in Ref. [37].

3.1.2. Torrefaction

The detailed analysis of the torrefaction process is available in Ref. [37]. Table 1 synthesizes the most important results. The carbon content increased after torrefaction, while the oxygen content decreased. Consequently, the HHV increased from 18.4 to 19.5 MJ.kg^{-1} on dry basis (Table 1). The main dry gases produced by the torrefaction are CO_2 and, to a lesser extent, CO. The mass fractions of CO_2 and CO in the dry gases are 0.81 and 0.18 respectively. Low amounts of H_2, CH_4, C_2H_2, C_2H_4, C_2H_6 and C_2H_8 are also found in permanent gases. The amount and the energy content of the released condensable species have been obtained by closing the mass and energy balances respectively. By closing the energy balance, the power of the torrefaction gases, including both condensable and dry gases, is estimated to be 13 kW for an inlet flow rate of biomass of 58 kg.h^{-1} on dry basis.

By closing the global energy balance of torrefaction, the net energy requirement is 178 kWh.tdb^{-1}. The total energy consumption is 621 kWh.tdb^{-1} (Table 2).

3.1.3. Post-combustion of the torrefaction gases and heat recovery

The detailed analysis of the post-combustion step and the heat recovery step are available in Ref. [37]. The following items synthesize the more important outcomes. The power supplied by natural gas slightly increased from 104 kW to 108 kW after the introduction of wood chips inside the torrefaction furnace. By closing the energy balance when torrefaction occurs, it is found that the reactive torrefaction gases act as a complementary fuel of the natural gas to supply energy to the post-combustion step. The total energy required for post-combustion is 2086 kWh.tdb^{-1}. 1861 kWh.tdb^{-1} are supplied by the burner (Table 2)

Table 2
Summary of the energy required for each step, per ton of input dry biomass. The indicated values are the mean values. When available, the standard deviations are indicated between parentheses. Note that the energy supplied by torrefaction gases in the post-combustion unit is not considered.

Pretreatment chains	Energy consumption (kWh.tdb^{-1})	Drying *		Torrefaction*	Post-combustion (gas cleaning step)*	Knife grinding	Vibratory milling
		From 52 % to 18 %	From 18 % to 11 %				
Drying + Grinding	Total	596 (4)	68	–	–	112 (3)	
	Net	594 (2)	68	–	–	62 (3)	
Drying + Torrefaction + Grinding	Total	596 (4)	68	621 (108)	1861 (146)	42 (1)	
	Net	594 (2)	68	178 (20)	55 (111)	27 (1)	
Drying + Grinding + Vibratory mill	Total	596 (4)	68	–	–	112 (3)	624
	Net	594 (2)	68	–	–	62 (3)	7

*More details are provided in [37].

and 225 kWh.tdb^{-1} are supplied by the combustion of torrefaction gases. The power recovered from the hot combustion gases through the heat exchanger is 111 kW, which corresponds to 1927 kWh.tdb^{-1}. It represents nearly 93 % of the energy supplied by natural gas and torrefaction gases in post-combustion.

3.1.4. Knife mill grinding

The net and total grinding indices for the knife milling of raw and torrefied wood are plotted in Fig. 4. The grinding of raw and torrefied woods to produce particles smaller than 1 mm requires respectively 92 kWh.tdb^{-1} and 30 kWh.tdb^{-1} in net basis (165 kWh.tdb^{-1} and 46 kWh.tdb^{-1} in total basis respectively). In this study, torrefaction has decreased the net grinding index by a factor 3.1 and the total grinding index by a factor 3.6.

Note that the grinding index also considers the size of particles as defined in section 2.4. Therefore, the net grinding energy is used instead to compare this study with the literature. In this study, the net grinding energy decreases by a factor 2.3 after torrefaction (Table 2). Similar results are found in the literature with resinous wood at similar torrefaction severity [54–56]. Strandberg et al. studied the grindability of spruce with a laboratory centrifugal mill. They reported a reduction of the net grinding energy by a factor 2.4 after a mildly torrefaction at pilot scale (11 % mass loss) [54]. Phanphanich et al. studied the grinding of raw and mildly torrefied pine (11 % mass loss) with a lab scale knife mill. They measured a decrease of the net grinding energy by 2.3 after torrefaction [55]. Kokko et al. showed that the net grinding energy cost of Scottish pine with a lab scale centrifugal mill decreases by a factor 2 after a torrefaction at 250 °C for 60 min (7 % mass loss) [56].

The decrease of the grinding energy cost after torrefaction is widely documented in the literature [4,27]. It is mainly attributed to the degradation of hemicelluloses, which are significantly contributing to the mechanical strength of the cell walls. After torrefaction, the cellulose fibers are more easily breakable due to the destruction of the matrix of hemicelluloses [24].

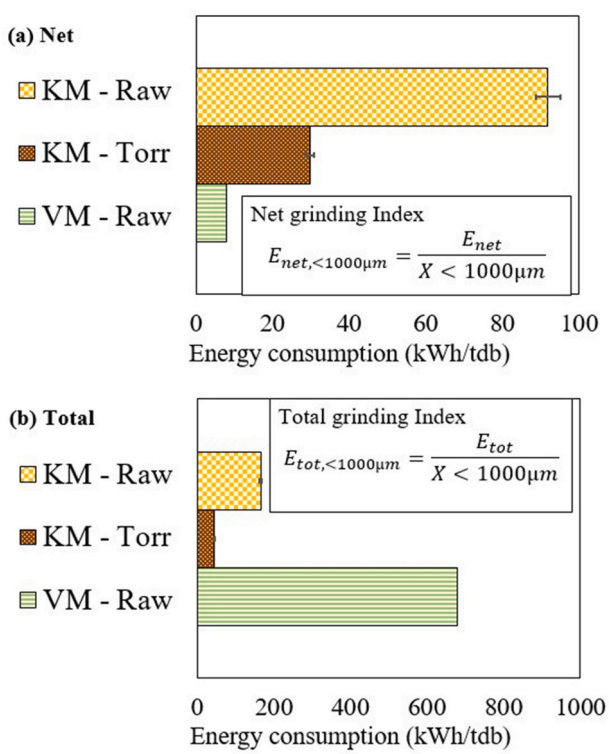

Fig. 4. **(a)** Net and **(b)** Total grinding indices of knife milling of raw wood (KM - Raw), knife milling of torrefied wood (KM - Torr) and fine grinding of the raw wood powder with the vibration mill (VM - Raw). Note that the latter considers only the vibratory mill step. Note also that the sieving energy cost is not considered.

3.1.5. Vibration mill grinding

A part of the powder of raw wood ground in the knife mill has undergone a second step of grinding in the vibration mill. The net grinding index for this additional grinding step is 8 kWh.tdb^{-1} and the total grinding index is 680 kWh.tdb^{-1} (Fig. 4). Compared with the other devices used in this work, this equipment is undersized in terms of capacity. In addition, as explained above, the feeding rate of wood powder has to be lowered to avoid the formation of arches at the chamber entrance. Therefore, it is not possible to perform measurements at the same flow rate as with the other devices. Consequently, the mass of powder inside the grinding chamber is small (about 0.1 kg) in comparison with the mass of the grinding media (about 70 kg). The power required to vibrate the grinding chamber is almost not affected by the presence of powder. It explains the so little value measured for the net energy consumption.

3.2. Material properties

3.2.1. Influence of torrefaction on the particle morphology after grinding

Fig. 5 shows the cumulative particle size distribution for the powder of raw wood (RWP), the powder of torrefied wood (TWP) and the powder of raw wood ground in the vibration mill (RWVP). These measurements have been performed after the sieving step (with a 1 mm screen). The size reported on the x-axis corresponds to the particle width.

The median particle diameter of RWP and TWP are respectively 662 μm and 264 μm. Torrefaction not only reduced the grinding energy cost but also decreased by half the particle diameter. This result agrees with previous findings [26,29,32]. The median particle diameter of RWVP is 220 μm. Some particles larger than 1000 μm still remain in the sieved fractions for the three powders. For example, 18 % of particles in volume in RWP are larger than 1000 μm. It could be explained by the geometry of the sieving screen. The side length of a square hole of the sieve is 1000 μm. However, some particles can pass through the sieve in the

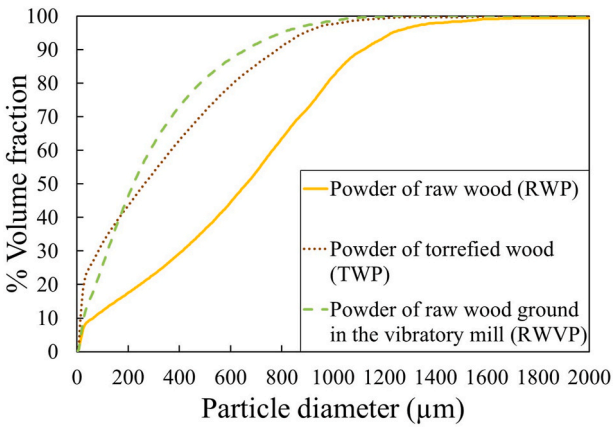

Fig. 5. Particle size distribution in the powders of raw and torrefied woods, and in the powder of raw wood ground in the vibration mill, after sieving at 1000 µm.

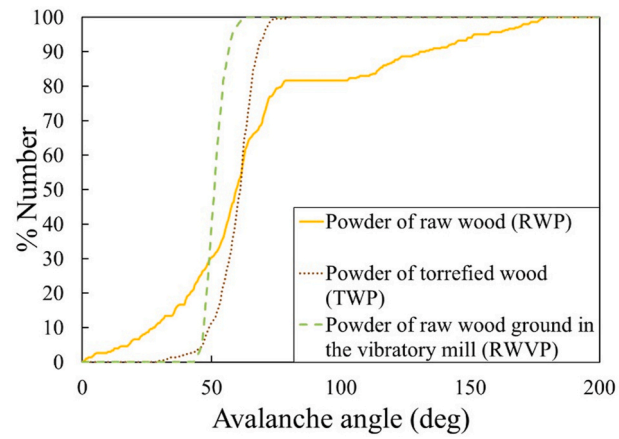

Fig. 6. Distribution of the avalanche angles for the 3 powders: RWP, TWP and RWVP.

direction of the hole diagonal, which measures $\sqrt{2}*1000 \approx 1410\ \mu m$. Indeed, there is almost no particle larger than 1400 µm as can be seen in Fig. 5.

The content of fines (particles smaller than 100 µm) in TWP is almost three times higher than that in the sieved fraction of RWP, respectively 32 % and 12 %. The content of fines in RWVP is 26 %.

The mean aspect ratio of the particles from RWP and TWP is respectively 0.41 and 0.48, after sieving. Thus, on average, the particles of TWP are a bit rounder than the particles of RWP. It may be explained by the greater number of fines in TWP compared to RWP. Indeed, Guo et al. observed a decrease of the aspect ratio with the increase of the average diameter of particles for several biomass powders (including pine wood) [7]. Furthermore, Phanphanich et al. found that the sphericity of particles of ground pine chips increased from 0.48 to 0.51 after torrefaction at 250 °C, and up to 0.60 after torrefaction at 275 °C. They concluded that the torrefaction improves the sphericity of ground particles under more severe conditions [55]. In this study, the severity of the torrefaction process was probably not enough to significantly change the particles shape.

The mean aspect ratio of the RWVP particles is found to be 0.65, which represents a significant improvement of the particle sphericity. It is even concluded that, from the sole point of view of the particle shape, the use of the vibratory mill has been more efficient than the rather mild torrefaction that has been operated here.

3.2.2. *Flowability of the wood powders in rotating drum*

The cumulative distributions of the avalanche angles of the three powders of this work are plotted in Fig. 6. The median avalanche angle is 60° for RWP, 61° for TWP and 52° for RWVP. RWP and TWP both have a high avalanche angle, but the distribution is much tighter for TWP. The standard deviation of avalanche angle values is respectively 8° and 39° for TWP and RWP.

With the powder of raw wood, some avalanche angles are found to be higher than 90°. It is due to the presence of agglomerates on the top of the powder bed that have held while the drum was rotating. This is a clear indication that this powder does sometimes flow under the form of agglomerates, which can for example cause irregular feeding rates in a process. Furthermore, this observation shows that the powder is cohesive, even when unconfined. Fig. 7 shows pictures of the powder surface just before the avalanche. The agglomerate of particles can be seen on the picture of raw wood powder (Fig. 7a.). Interestingly, the avalanche angles of TWP and RWVP never exceed 90°. They have a distribution around their median value, respectively 61 ± 8° and 52 ± 4°. It thus shows that both treatments have efficiently reduced the cohesion of the powders allowing them to flow inside the drum quite similarly to a non-cohesive material. From these results, the powder ground in the vibration mill has the most favorable characteristics and should then have the best flowability under no stress. Torrefaction has also improved the powder flowability, but to a lesser extent than the vibration mill.

3.2.3. *Shear tests*

The mechanical resistance under shearing of the different wood powders produced in this study has bee$\varepsilon_t^{'}$n investigated in a Schulze shear cell. The experiments have been performed with the powders sieved at 1000 µm.

Fig. 8 displays three graphs for RWP, TWP and RWVP, where the prorated (see eq. (5)) yield shear stress $\tau_s^{'}$ is plotted versus the normal stress σ for four different normal preconsolidation stress σ_c (symbols). All the stresses are dimensionally reduced by the preconsolidation stress. This scaling leads the four yield loci to collapse in a single curve which has been fitted by the Warren-Spring model (thick black line). This method of simplification is supported by Williams and Birks [57], who showed with dry powders that all the reduced shear stresses obtained under different preconsolidation stresses lie well on the same curve [57]. The reduced Major Consolidation Stress (σ_1/σ_c) and the reduced Unconfined Yield Strength (f_C/σ_c) are indicated in Fig. 8 (red-thick or blue-dotted Mohr circles), and are 2.95 and 0.32 for RWP, 3.02 and 0.15 for TWP and 2.69 and 0.16 for RWVP, respectively. The Unconfined Yield Strength is the minimal stress required to fracture a consolidated material to start the flow. The stress needed to break a cohesive arch is much lower for TWP and RWVP. As mentioned in section 2.3.4, the ratio ffc is an indicator of powder flowability under mechanical constraint. The larger ffc is, the better the powder flows. The ratio ffc is 9, 20 and 17 for RWP, TWP and RWVP, respectively. The improvement of flowability caused by torrefaction has been already highlighted by Pachón-Morales et al. They attribute this to the reduction of the length over width ratio as well as to the decreased roughness of particle surfaces [29]. In this study, the aspect ratio of the particles has not been changed a lot after torrefaction (see section 3.2.1). Thus, the flowability improvement is preferably explained by the smoothing of particle surfaces due to the heat treatment.

The vibratory mill has improved the wood powder flowability in an equivalent extent than torrefaction. The surfaces of wood particles before and after grinding in the vibration mill have not been investigated in this work, so it is not possible to know whether the roughness of wood particles has been changed. Nevertheless, it is observed in section 3.2.1 that the aspect ratio of particles ground in the vibratory mill has been enhanced, which could at least partly explain why the flowability has been enhanced.

The results presented in this section show that a pretreatment step such as torrefaction or vibratory milling improves significantly the

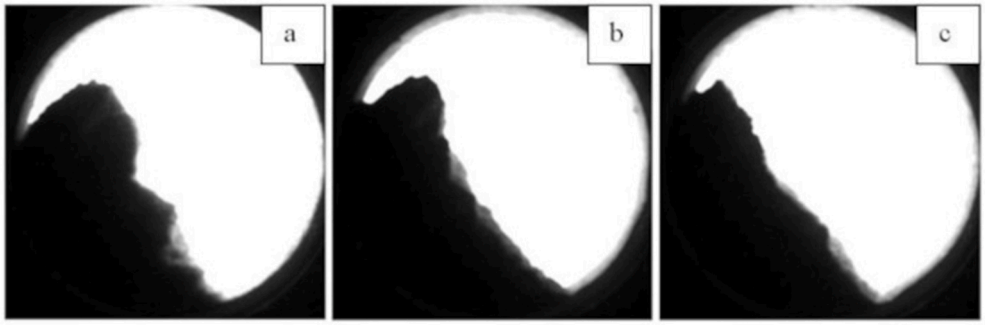

Fig. 7. Shape of the powder surface before an avalanche for the **(a)** powder of raw wood (RWP), **(b)** powder of torrefied wood (TWP) and **(c)** powder of raw wood ground in the vibratory mill (RWVP).

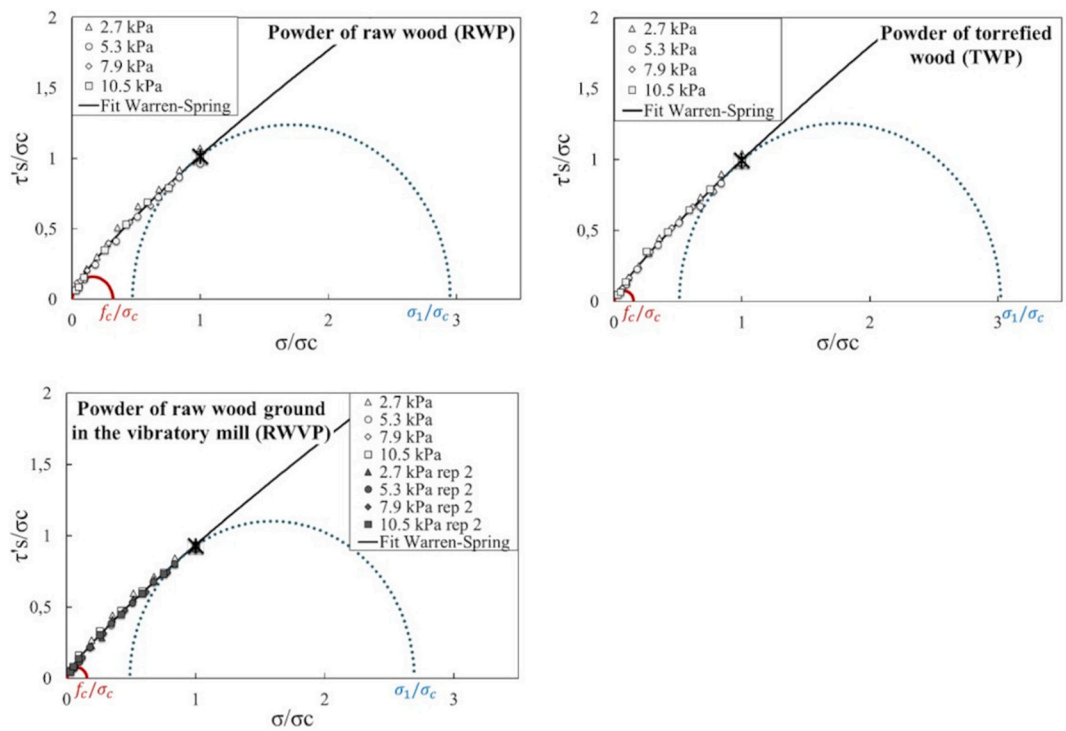

Fig. 8. Reduced yield loci of the powders of raw wood (RWP), of torrefied wood (TWP) and of raw wood ground in the vibration mill (RWVP), with associated Warren-spring fit and Mohr circles. The larger Mohr circle is plotted with a blue dotted line and the smaller Mohr circle is plotted with a continuous red line. The preconsolidation point is plotted with a black cross. The reduced Unconfined Yield Strength f_c/σ_c and the reduced Major Consolidation Stress σ_1/σ_c are indicated in red and in blue, respectively. (For interpretation of the references to colour in this figure legend, the reader is referred to the Web version of this article.)

flowability of wood powders.

3.3. Energy and biomass feedstock requirements in the considered pretreatment chains

3.3.1. Detailed mapping of the energy and mass balances

Fig. 9 shows the different steps of the four considered pretreatment chains: DG (Drying + Grinding), DTG (Drying + Torrefaction + Grinding), DGV (Drying + Grinding + Vibratory mill) and DTG + Hi (Drying + Torrefaction + Grinding with Heat integration). Mass and total energy fluxes are given for each step to produce one ton of dry powder at required size (particles smaller than 1000 μm). Note that in the grinding steps, the oversized particles are re-injected in the grinder.

The total energy requirements to produce one ton of each dry product are plotted in Fig. 10. The energy required for sieving has not been measured. Even if torrefaction reduces the total grinding index by a factor 3.6, the total energy requirements of the whole chain are high in comparison with the other chains. As expected, the lowest energy cost of production is obtained for the DG chain. By comparison, the DTG and DGV chains have respectively an extra cost of 2730 kWh.tdb^{-1} and 626 kWh.tdb^{-1}. It represents respectively 58 % and 13 % of the LHV of biomass.

The main energy requirement in the DTG chain is the post treatment of torrefaction gases. The energy cost of the post-combustion represents nearly 58 % of the total energy cost of the DTG chain. Note that, as previously mentioned, the energy required for post-combustion presented in Fig. 9 and in Fig. 10 only take into account the energy supplied by natural gas. The difference in the energy requirements of DTG and DTG + Hi chains clearly highlights the need of recovering energy downstream the post-combustion. Heat integration should thus be implemented to increase the overall efficiency of any chain including a torrefaction stage [35,36].

In this study, the energy of the flue gases exiting the post-combustion unit is recovered via a fumes/air heat exchanger. The post-combustion of torrefaction gases must be operated with an excess of oxygen, as required by the French regulation, to ensure a complete oxidation of any

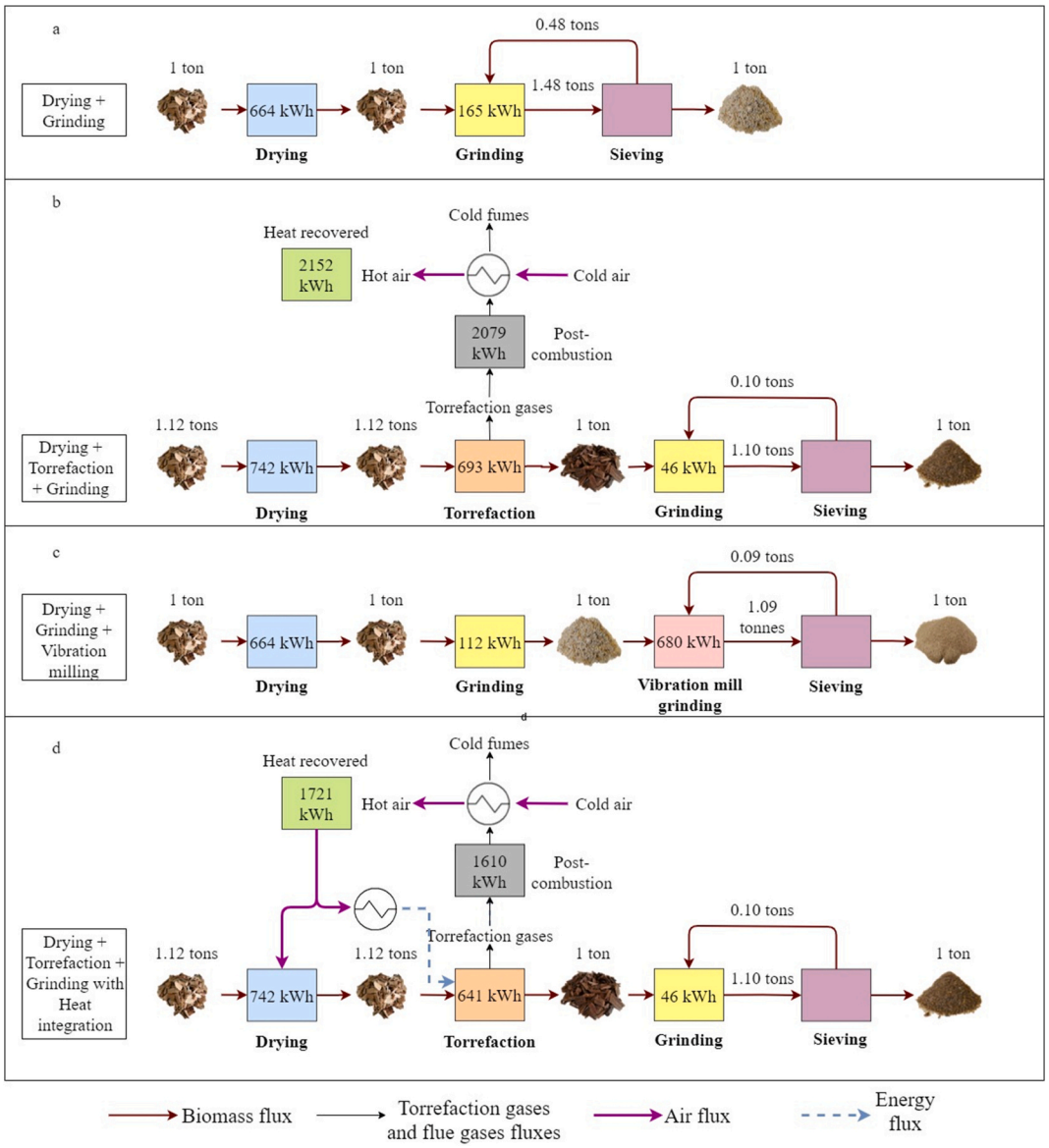

Fig. 9. Overview of the four considered pre-treatment chains: (a) DG, (b) DTG, (c) DGV and (d) DTG + Hi. The mass fluxes are represented with continuous lines and the thermal fluxes are represented with dotted lines.

species in the fumes. In our installation, the oxygen level in the gas exiting the post-combustion reactor is set at 5%vol. Therefore, this gas cannot be directly injected in the torrefaction furnace, and the recovery of its energy content for supplying the torrefaction process has to be carried out via a heat exchanger. Obviously, the amount of energy recovered after the heat exchanger depends on the efficiency of the installation.

It has already been demonstrated in Ref. [37] that the energy recovered in the post-combustion gases can supply the whole energy for drying and torrefaction. Note that the latter is assumed to be indirectly heated up, as air cannot be introduced in the torrefaction furnace. Two main technologies of reactors with indirect heating are distinguished in the literature: auger and rotary type [58]. In both cases, energy is provided by heat exchangers inside the reactor [58]. A possible scenario whereby the torrefaction reactor is indirectly heated up is presented in Fig. 9. It is the DTG + Hi chain.

All the details of the data used in such a scenario are provided in Ref. [37]. The more important observation is that the dry and the condensable torrefaction gases cannot provide enough energy to the post-combustion, thus an auxiliary fuel is needed. The complementary fuel flow rate has been calculated by closing the energy balance for the post-combustion step. It is in accordance with the conclusions of Haseli [59]. Haseli developed a model to simulate the performance of a torrefaction unit. He concluded that a torrefaction plant processing with spruce at a torrefaction temperature lower than 300 °C would need an extra fuel to be burnt (in addition to the volatiles) [59].

The total energy requirement of the torrefaction process with heat integration to produce one ton of torrefied powder is 1656 kWh (Fig. 10). Heat integration decreases by half the energy cost of the DTG chain. A torrefaction process with heat integration requires slightly more energy than a chain including a vibratory mill. The energy cost of all the chains could be further decreased with the use of a Vapor Re Compression system to recover the heat of evaporation in the drying process [60].

3.3.2. *Wood chips requirements*

In a sustainable process, the natural gas should be replaced by biomass. Therefore, calculations have been made to assess the amount of wet wood chips (i.e. as received) required to produce powder and to supply heat to the process via combustion in a boiler. The energy

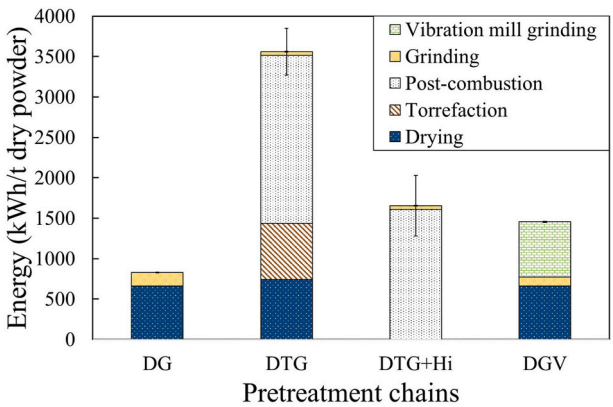

Fig. 10. Overall energy supplied from external sources of energy for the considered pre-treatment chains: DG (Drying + Grinding), DTG (Drying + Torrefaction + Grinding), DTG + Hi (Drying + Torrefaction + Grinding with Heat integration) and DGV (Drying + Grinding + Vibration mill). The external sources of energy are natural gas for drying, torrefaction and post-combustion, and electricity for grinding.

released by the combustion of wood has been assessed using the heat content of raw or torrefied woods presented in Table 1. The efficiency of the boiler has been assumed to be 90 % [61]. In such a process, there are a priori three options to feed the boiler: with wet wood chips with a moisture content of 52 % on a wet basis (configuration n°1), with dried wood chips with a moisture content of 11 %wb (configuration n°2), or with torrefied wood chips (configuration n°3). Each option has been investigated. The energy required to prepare the dried wood chips and the torrefied wood chips to feed the boiler in the configuration n°2 and in the configuration n°3 respectively has been taken into account based on the energy required for each step indicated in Table 2. Obviously, this excess of energy is also assumed to be supplied by combustion of biomass. Therefore, the wet wood chips requirements for heat production have been determined by closing the energy and mass balances. The results are shown in Fig. 11.

In the configuration n°1, the wet biomass requirements range from 2.5 tons in the DG and DGV chains up to 4.3 tons in the DTG chain. Requirements are reduced down to 3.3 tons in the DTG + Hi chain. Similar results are found with the configuration n°2. With the latter, the wet biomass requirements vary from 2.5 tons in the DG and DGV chains up to 4.4 tons in the DTG chain. In the DTG + Hi chain, the wet biomass requirements are reduced to 3.2 tons. Lastly, the configuration n°3 has the highest wood chips requirements. The DTG and DTG + Hi chains

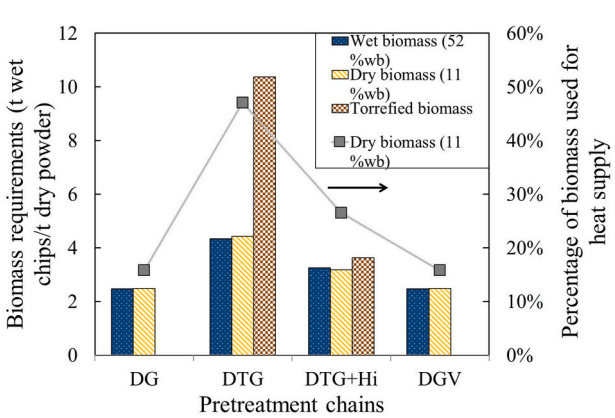

Fig. 11. Wood requirements (under the form of wet chips, as received) to produce one ton of dry powder and to supply energy to the process from combustion of wet biomass, of dry biomass and of torrefied biomass. The curve indicates the percentage of biomass used for heat production in the configuration n°2 (dried wood chips (11 %wb) are used as feedstock in the boiler).

require respectively 10.4 and 3.6 tons of wet wood chips. Note that for all the configurations, a special attention has been paid to the chain DTG + Hi, to verify that the energy recovered from the gases exiting the post-combustion meets well the energy requirements of both the drying and torrefaction units.

It is worth noting that the thermal efficiency of any boiler may decrease when increasing the moisture content of firewood [62]. The efficiency of 90 % might be overestimated with wet feedstock. Considering the above, the use of dry biomass as feedstock for combustion might be the best compromise (configuration n°2).

The curve with squares in Fig. 11 indicates the percentage of wet biomass chips used in the boiler to supply heat to the process in the configuration n°2. In the DG chain, most of the wet wood chips are processed into powder (84 %), the rest being used to supply heat to produce the powder and to dry the chips feeding the boiler (16 %). Similar results are found in the DGV chain because the extra energy due to the use of the vibration mill is electricity and not heat. In all the chains, more than 50 % of the wood chips used in the process are transformed as powder.

To produce one ton of dry powder to feed an EFR unit, between 2.5 and 4.4 tons of biomass must be transported from loggings to the process plant. Besides the economic cost of transport, it would have non negligible CO_2 emissions. The development of decentralized process units could be a way to limit the cost. In this concept, the use of torrefaction could be fully justified. According to Magalhães et al. decentralized torrefaction units are more cost-effective and more ecological in terms of CO_2 emissions than centralized plants [63].

3.4. Synthesis

Fig. 12 gives a comparative overview of some properties of the powders. The costs in energy and in biomass are plotted in this graph as well, to better highlight the advantages and the drawbacks of each chain of production considered in this work. The properties presented in Fig. 12 are the morphology of particles and the flowability of the powders under free surface conditions and under consolidation. The data are normalized by the values corresponding to the coarse raw powder (RWP). The green dotted arrows indicate that a high value is beneficial for the gasification process while the red arrows mean that a high value is disadvantageous.

Regarding the unconfined flow of powder, the route with the

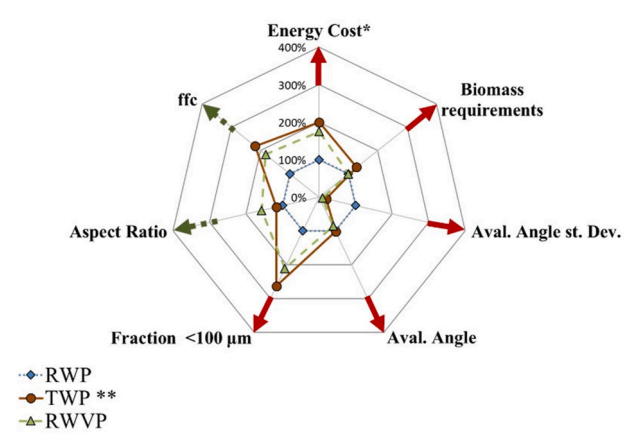

Fig. 12. Comparative overview of the main characteristics of the sieved powders (RWP, TWP and RWVP) and their respective costs. Note that all the data plotted in this graph are normalized by the corresponding values of the powder made of raw wood ground in the knife mill - * the energy consumption plotted here does not consider the electricity consumption needed to operate the dryer and the central shaft of the torrefaction furnace - ** The energy and biomass costs of the torrefied powder are those of a heat integrated torrefaction plant (see section 3.3.1.).

vibration mill appears to be the best choice. The resulting powder has the lowest median avalanche angle and the tightest distribution of avalanche angles. But the powder manufactured with torrefied wood has comparable results. Taking into consideration the flowability of powders when consolidated by a vertical stress, the powder of torrefied wood represents the "best" product made in this work. If the energy cost is the most important criterion, the raw biomass ground in the knife mill is the least expensive product. Powders of raw wood have the lowest feedstock requirements. Regarding the safety issues, the content of fines is of primary importance with this kind of combustible materials; the least proportion of fines is found in the powder made of raw wood ground with the knife mill.

The properties of the powders considered here are some quantitative characteristics measurable with laboratory devices. Some of them are directly relevant for any process of valorization, like the content of fines. But most of these data only enable to compare the powders towards the risk of occurrence of different issues, e.g. clogging, fouling, unstable feeding rates … The knowledge of these different characteristics is ineffective to assure that a process of gasification will run correctly with any of the powders. This question will be the subject of a forthcoming work, by observing how the different powders behave in pilot sized devices of storage and of injection.

4. Conclusions

In this study, wood powders have been produced from resinous wood chips at pilot scale. Four different chains of production have been compared, based on their energy requirements as well as the flowability of the powders.

The pretreatment chain including only drying and coarse grinding requires the least energy. However, the ability of this powder to flow either without any stress or when consolidated by a vertical stress is low. Thus, this powder is not expected to flow well at industrial scale. Mild torrefaction and vibration mill both improve significantly the flowability of wood powders to a similar extent. Even though torrefaction significantly reduces the grinding energy, the energy requirements of the whole process are still much higher than for the chain including a vibration mill. This high energy cost is mainly due to the post-combustion of torrefaction gases. Recovering the heat of the gases downstream the post-combustion enables to decrease by half the total energy requirement and by a quarter the resource requirements.

Though we have obtained here some results enabling to compare the flowability of various wood powders, this knowledge is still insufficient to predict how they will behave in an industrial plant. The study of their behaviour during injection and storage in pilot-scale devices will be the subject of forthcoming works.

Acknowledgements

This work was supported by the French Environment and Energy Management Agency (ADEME) and CEA. The French agency for research (ANR) is acknowledged for partial funding of the GENEPI platform within the framework of the investments of future (Ref: ANR-11-EQPX-0019).

The authors thank Hélène Miller from CEA Liten for elementary and calorimetry analyses of raw and torrefied woods, Göknur Esra Hasbay for her contribution in the characterization of powders in shear cell and Thierry Chataing from CEA Liten for the helpful discussion about post-combustion.

Appendix A

The experimental data collected during each step of the preparation of wood powders are summarized in Table A.1.

Table A.1
Summary of the experimental data for each step. When the measurements have been repeated, the mean value is indicated with the standard deviation between parentheses

Parameters	Mean value (standard deviation)	
Drying		
Inlet moisture content (%)	52 (2.6)	
Residence time (min)	78	
Inlet flow rate of biomass (kg.h-1)	117	
Burner power (kW)	33 (0.2)	
Outlet flow rate of biomass (kg.h-1)	75 (0.2)	
Flow rate of evaporated water (kg.h-1)	42 (0.2)	
Moisture content of wood at the outlet (%)	18 (0.5)	
Torrefaction		
Moisture content of wood at the inlet (%)	11 (1.8)	
Inlet flow rate of biomass (kg.h-1)	65 (1.2)	
Outlet flow rate of biomass (kg.h-1)	52 (0.1)	
Mass yield (%)	89.6 (0.0)	
Energy yield (%)	95.3 (0.0)	
Burners power, empty furnace (kW)	28 (5.7)	
Burners power, full furnace (kW)	36 (6.2)	
Post-combustion		
Reactor temperature (°C)	1000	
Burner power, empty reactor (kW)	104 (1.8)	
Burner power, with load (kW)	108 (8.3)	
Heat exchanger		
Air temperature at the inlet (°C)	29 (4.2)	
Air temperature at the outlet (°C)	134 (9.9)	
Knife grinding	**Raw wood**	**Torrefied wood**
Inlet flow rate of biomass (kg.h-1)	59 (1.7)	181 (11.4)
Moisture content of wood at the inlet (%)	12 (0.0)	6 (0.3)
Grinder power when empty (kW)	2.6 (0.1)	2.5 (0.1)
Grinder power with load (kW)	5.8 (0.2)	7.1 (0.3)
Vibratory milling		

(*continued on next page*)

Table A.1 (*continued*)

Parameters	Mean value (standard deviation)
Inlet flow rate of biomass (kg.h-1)	1.8
Moisture content of wood at the inlet (%)	10 (0.1)
Grinder power when empty (kW)	1.00
Grinder power with load (kW)	1.01

Table A.2 presents the values of the Unconfined Yield Strength, Major Consolidation Stress, flowability factor, cohesion and effective angle of internal friction resulting from the Schulze shear cell tests. The values are dependent on the preconsolidation stress.

Table A.2
Flow properties of the powder of raw wood (RWP), the powder of torrefied wood (TWP) and the powder of raw wood ground in the vibration mill (RWVP) at four preconsolidation stresses: 2.7 kPa, 5.3 kPa, 7.9 kPa and 10.5 kPa. Note that the experiments performed with RWVP have been duplicated

	Preconsolidation stress (kPa)	RWP	TWP	RWVP	RWVP –duplicate
Unconfined Yield Strength, f_C (kPa)	2.7	1.377	0.723	0.630	0.339
	5.3	0.834	0.776	0.533	0.497
	7.9	3.245	1.082	1.130	0.969
	10.5	2.513	1.485	2.606	1.846
Major Consolidation Stress, σ_1 (kPa)	2.7	6.909	6.932	6.819	6.686
	5.3	12.225	12.764	12.785	12.861
	7.9	19.239	20.258	19.055	18.994
	10.5	25.255	25.621	25.941	25.601
Flowability factor, *FFC*	2.7	5.0	9.6	10.8	19.7
	5.3	14.7	16.4	24.0	25.9
	7.9	5.9	18.7	16.9	19.6
	10.5	10.0	17.3	10.0	13.9
Cohesion, *C* (kPa)	2.7	0.229	0.133	0.092	0.054
	5.3	0.112	0.139	0.085	0.077
	7.9	0.583	0.150	0.189	0.168
	10.5	0.335	0.194	0.413	0.307
Effective angle of internal friction, ϕ_e (°)	2.7	49.5	47.5	45.7	44.5
	5.3	46.9	45.7	44.3	44.4
	7.9	47.3	45.2	43.4	43.7
	10.5	47.9	46.6	44.5	43.8

References

[1] IEA, World Energy Balances: Overview, 2019.
[2] I.D. Suckling, Production of biofuels from lignocellulosic biomass: an overview of the conversion technologies, Appita J. 67 (2014) 97–105.
[3] J. Billaud, S. Valin, G. Ratel, M. Peyrot, F. Weiland, H. Hedman, S. Salvador, Biomass gasification in entrained flow reactor: influence of wood particle size, Chem. Eng. Trans. 50 (2016) 37–42.
[4] P. Karinkanta, A. Ämmälä, M. Illikainen, J. Niinimäki, Fine grinding of wood – overview from wood breakage to applications, Biomass Bioenergy 113 (2018) 31–44.
[5] J. Visser, An invited review Van der Waals and other cohesive forces affecting powder fluidization, Powder Technol. 58 (1989) 1–10.
[6] C. Vanneste-Ibarcq, Study of Biomass Powders in the Context of Thermal Recovery Processes, PhD Thesis, Université de Toulouse, 2018.
[7] Q. Guo, X. Chen, H. Liu, Experimental research on shape and size distribution of biomass particle, Fuel 94 (2012) 551–555.
[8] R.P.K. Ambrose, S. Jan, K. Siliveru, A review on flow characterization methods for cereal grain-based powders, J. Sci. Food Agric. 96 (2016) 359–364.
[9] G. Xu, P. Lu, M. Li, C. Liang, P. Xu, D. Liu, X. Chen, Investigation on characterization of powder flowability using different testing methods, Exp. Therm. Fluid Sci. 92 (2018) 390–401.
[10] A. Castellanos, J.M. Valverde, M.A.S. Quintanilla, Fine cohesive powders in rotating drums: transition from rigid-plastic flow to gas-fluidized regime, Phys. Rev. E 65 (2002), 061301.
[11] A.W. Alexander, B. Chaudhuri, A.M. Faqih, F.J. Muzzio, C. Davies, M. S. Tomassone, Avalanching flow of cohesive powders, Powder Technol. 164 (2006) 13–21.
[12] A.M. Faqih, A. Mehrotra, B. Chaudhuri, M. Silvina Tomassone, F.J. Muzzio, A method for predicting hopper flow characteristics of unconfined cohesive powders, AIChE Annual Meeting, Conference Proceedings (2005) 2933.
[13] D. Schulze, Powders and Bulk Solids: Behavior, Characterization, Storage and Flow, first ed., Springer, 2008.
[14] K. Svoboda, M. Pohořelý, M. Hartman, J. Martinec, Pretreatment and feeding of biomass for pressurized entrained flow gasification, Fuel Process. Technol. 90 (2009) 629–635.
[15] J.S. Tumuluru, S. Sokhansanj, J.R. Hess, C.T. Wright, R.D. Boardman, A review on biomass torrefaction process and product properties for energy applications, Ind. Biotechnol. 7 (2011) 384–401.
[16] A.E. Eseyin, P.H. Steele, C.U. Pittman Jr., Current trends in the production and applications of torrefied wood/biomass - a review, BioResources 10 (2015) 8812–8858.
[17] M. Hakkou, M. Pétrissans, P. Gérardin, A. Zoulalian, Investigations of the reasons for fungal durability of heat-treated beech wood, Polym. Degrad. Stabil. 91 (2006) 393–397.
[18] V.R. de Castro, M.P. de Castro Freitas, A.J.V. Zanuncio, J.C. Zanuncio, P.G. Surdi, A.C.O. Carneiro, B.R. Vital, Resistance of in natura and torrefied wood chips to xylophage fungi, Sci. Rep. 9 (2019).
[19] W.-H. Chen, C.-J. Chen, C.-I. Hung, C.-H. Shen, H.-W. Hsu, A comparison of gasification phenomena among raw biomass, torrefied biomass and coal in an entrained-flow reactor, Appl. Energy 112 (2013) 421–430.
[20] F. Weiland, M. Nordwaeger, I. Olofsson, H. Wiinikka, A. Nordin, Entrained flow gasification of torrefied wood residues, Fuel Process. Technol. 125 (2014) 51–58.
[21] C. Berrueco, J. Recari, B.M. Güell, G. del Alamo, Pressurized gasification of torrefied woody biomass in a lab scale fluidized bed, Energy 70 (2014) 68–78.
[22] Y. Mei, R. Liu, Q. Yang, H. Yang, J. Shao, C. Draper, S. Zhang, H. Chen, Torrefaction of cedarwood in a pilot scale rotary kiln and the influence of industrial flue gas, Bioresour. Technol. 177 (2015) 355–360.
[23] R. Junga, J. Pospolita, P. Niemiec, Combustion and grindability characteristics of palm kernel shells torrefied in a pilot-scale installation, Renew. Energy 147 (2020) 1239–1250.
[24] P.C.A. Bergman, A.R. Boersma, J.H.A. Kiel, M.J. Prins, K.J. Ptasinski, F.J.J. G. Janssen, Torrefaction for Entrained-Flow Gasification of Biomass, 2005.
[25] V. Repellin, A. Govin, M. Rolland, R. Guyonnet, Energy requirement for fine grinding of torrefied wood, Biomass Bioenergy 34 (2010) 923–930.
[26] B. Colin, J.-L. Dirion, P. Arlabosse, S. Salvador, Quantification of the torrefaction effects on the grindability and the hygroscopicity of wood chips, Fuel 197 (2017) 232–239.
[27] C. Mayer-Laigle, R.K. Rajaonarivony, N. Blanc, X. Rouau, Comminution of dry lignocellulosic biomass: Part II. technologies, improvement of milling performances, and security issues, Bioengineering 5 (2018).
[28] M. Almendros, O. Bonnefoy, A. Govin, W. Nastoll, E. Sanz, R. Andreux, R. Guyonnet, Influence of Torrefaction Treatment on Wood Powder Properties, in: 19th European Biomass Conference, ETA-Florence Renewable Energies, Berlin, Germany, 2011, pp. 1902–1904.
[29] J. Pachón-Morales, J. Colin, F. Pierre, F. Puel, P. Perré, Effect of torrefaction intensity on the flow properties of lignocellulosic biomass powders, Biomass Bioenergy 120 (2019) 301–312.

[30] G. Xu, M. Li, P. Lu, Experimental investigation on flow properties of different biomass and torrefied biomass powders, Biomass Bioenergy 122 (2019) 63–75.
[31] B. Arias, C. Pevida, J. Fermoso, M.G. Plaza, F. Rubiera, J.J. Pis, Influence of torrefaction on the grindability and reactivity of woody biomass, Fuel Process, Technol. 89 (2008) 169–175.
[32] A. Govin, V. Repellin, M. Rolland, J.-L. Duplan, Effect of Torrefaction on Grinding Energy Requirement for Thin Wood Particle Production, in: XII ° Congrès de La Société Française de Génie Des Procédés vol. 98, Société Fançaise de Génie des Procédés, Marseille, France, 2009.
[33] C. Di Blasi, M. Lanzetta, Intrinsic kinetics of isothermal xylan degradation in inert atmosphere, J. Anal. Appl. Pyrolysis 40–41 (1997) 287–303.
[34] W.-H. Chen, H.-C. Hsu, K.-M. Lu, W.-J. Lee, T.-C. Lin, Thermal pretreatment of wood (Lauan) block by torrefaction and its influence on the properties of the biomass, Energy 36 (2011) 3012–3021.
[35] P. Nanou, M.C. Carbo, J.H.A. Kiel, Detailed mapping of the mass and energy balance of a continuous biomass torrefaction plant, Biomass Bioenergy 89 (2016) 67–77.
[36] N. Doassans-Carrère, S. Muller, M. Mitzkat, REVE - a new industrial technology for biomass torrefaction: pilot studies, Fuel Process, Technol. 126 (2014) 155–162.
[37] F. Thevenon, M. Marchand, M. Grateau, H. Demey, A. Chatroux, A. De Ryck, T. Melkior, Continuous Torrefaction of Resinous Wood Chips in Multiple Hearths Furnace: Mass and Energy Balances, in: Proc. Of the Venice 2020, CISA Publisher, Venice, 2020.
[38] D. Ciolkosz, R. Wallace, A review of torrefaction for bioenergy feedstock production, Biofuels, Bioprod. Bioref. 5 (2011) 317–329.
[39] N. Kobayashi, P. Guilin, J. Kobayashi, S. Hatano, Y. Itaya, S. Mori, A new pulverized biomass utilization technology, Powder Technol. 180 (2008) 272–283.
[40] N. Kobayashi, Y. Itaya, Estimation of production and energy consumption in woody biomass pulverization using a multiple tube vibration mill, J. Chem. Eng. Process Technol. 6 (2015).
[41] T. Takahashi, Scaled-up pulverizing for lignocellulose biomass using a vibratory mill with ring media, Renew. Energy 144 (2019) 77–83.
[42] P. Karinkanta, M. Illikainen, J. Niinimäki, Effect of different impact events in fine grinding mills on the development of the physical properties of dried Norway spruce (Picea abies) wood in pulverisation, Powder Technol. 253 (2014) 352–359.
[43] H. Demey, T. Melkior, A. Chatroux, K. Attar, S. Thiery, H. Miller, M. Grateau, A. M. Sastre, M. Marchand, Evaluation of torrefied poplar-biomass as a low-cost sorbent for lead and terbium removal from aqueous solutions and energy co-generation, Chem. Eng. J. 361 (2019) 839–852.
[44] H. Demey, et al., Torrefaction of Wheat Straw and Sunflower Shells Biomasses as Low-Cost Materials for Energy Co-generation, in: M. Ksibi, et al. (Eds.), Recent Advances in Environmental Science from the Euro-Mediterranean and Surrounding Regions, second ed., Springer, Cham, 2021. EMCEI 2019. Environmental Science and Engineering.
[45] J. Ross Robert, Wood handbook : wood as an engineering material. Centennial Ed. General Technical Report FPL ; GTR-190, U.S. Dept. of Agriculture, Forest Service, Forest Products Laboratory, Madison, WI, 2010, 2010: 1 v.
[46] D. Maski, M.J. Darr, R.P. Anex, "Torrefaction of cellulosic biomass upgrading – energy and cost model", Agricultural and Biosystems Engineering Conference Proceedings and Presentations 6 (2010). http://lib.dr.iastate.edu/abe_eng_conf/291.
[47] AIDA, Arrêté du 03/08/18 relatif aux installations de combustion d'une puissance thermique nominale totale inférieure à 50 MW soumises à autorisation au titre des rubriques 2910, 2931 ou 3110 (applicable à compter du 20 décembre 2018), 2018 accessed in nov, https://aida.ineris.fr/consultation_document/41041.
[48] Y. Liu, H. Lu, M. Poletto, X. Guo, X. Gong, Y. Jin, Flow properties and inter-particle forces in fuel powders, Particuology 34 (2017) 24–38.
[49] J. Falk, R.J. Berry, M. Broström, S.H. Larsson, Mass flow and variability in screw feeding of biomass powders - relations to particle and bulk properties, Powder Technol. 276 (2015) 80–88.
[50] ASTM D6773-02: Standard Shear Test Method for Bulk Solids, Using the Schulze Ring Shear Tester, ASTM International, 2002.
[51] M.D. Ashton, D.C.-H. Cheng, R. Farley, F.H.H. Valentin, Some investigations into the strength and flow properties of powders, Rheol. Acta 4 (1965) 206–218.
[52] C. Vanneste-Ibarcq, T. Melkior, A. De Ryck, Warren-Spring based model for the shear yield locus of cohesive biomass powders, EPJ Web Conf. 140 (2017).
[53] M. Peleg, M.D. Normand, M.G. Corradini, Interactive software for calculating the principal stresses of compacted cohesive powders with the Warren-Spring equation, Powder Technol. 197 (2010) 268–273.
[54] M. Strandberg, I. Olofsson, L. Pommer, S. Wiklund-Lindström, K. Aberg, A. Nordin, Effects of temperature and residence time on continuous torrefaction of spruce wood, Fuel Process, Technol. 134 (2015) 387–398.
[55] M. Phanphanich, S. Mani, Impact of torrefaction on the grindability and fuel characteristics of forest biomass, Bioresour. Technol. 102 (2011) 1246–1253.
[56] L. Kokko, H. Tolvanen, K. Hämäläinen, R. Raiko, Comparing the energy required for fine grinding torrefied and fast heat treated pine, Biomass Bioenergy 42 (2012) 219–223.
[57] J.C. Williams, A.H. Birks, The comparison of the failure measurements of powders with theory, Powder Technol. 1 (1967) 199–206.
[58] Paweł Stępień, Jakub Pulka, Andrzej Białowiec, July 5th, Organic Waste Torrefaction – A Review: Reactor Systems, and the Biochar Properties, Pyrolysis, Mohamed Samer, IntechOpen, 2017, https://doi.org/10.5772/67644. Available from, https://www.intechopen.com/books/pyrolysis/organic-waste-torrefaction-a-review-reactor-systems-and-the-biochar-properties.
[59] Y. Haseli, Process modeling of a biomass torrefaction plant, Energy Fuels 32 (2018) 5611–5622.
[60] K. Kaminaka, Y. Matsumura, W. Noaman Omar, Y. Uemura, Process evaluation for torrefaction of empty fruit bunch in Malaysia, J. Japan Pet. Inst. 57 (2014) 88–93.
[61] P. Le Louer, R. Leclercq, A. Wanin, M. Force, G. Remond, A. Hachimi, Evaluation des performances énergétiques et environnementales de chaufferies biomasse, ADEME, 2014.
[62] L. Dzurenda, A. Banski, Influence of moisture content of combusted wood on the thermal efficiency of a boiler, Arch. Therm. 38 (2017) 63–74.
[63] A.I.P. Magalhães, D. Petrović, A.L. Rodriguez, Z.A. Putra, G. Thielemans, Techno-economic assessment of biomass pre-conversion processes as a part of biomass-to-liquids line-up, Biofuels, Bioprod. Bioref. 3 (2009) 584–600.